DFT AND DOCKING STUDY OF POTENTIAL TRANSITION STATE ANALOGUE INHIBITORS OF GLYCOSYLTRANSFERASES

Lucie SIHELNIKOVÁ[1], Stanislav KOZMON[2] and Igor TVAROŠKA[3,*]

Institute of Chemistry, Slovak Academy of Sciences, 845 38 Bratislava, Slovakia; e-mail: [1] chemsihl@savba.sk, [2] chemsksa@savba.sk, [3] chemitsa@savba.sk

Received March 6, 2008
Accepted April 17, 2008
Published online May 29, 2008

Conformational behavior of the [(2*S*,3*R*,4*R*,5*S*)-3,4,5-trihydroxy-2-(phenylsulfanyl)tetrahydrofuran-2-yl]methyl sulfate anion (**2**), which is the potential transition state (TS) analogue of the inverting glycosyltransferases, was studied by means of two-dimensional potential-energy maps, using a density functional theory method at the B3LYP/6-31+G* level. The maps revealed the presence of eight low-energy domains which were refined at the B3LYP/6-311++G** level and led to six conformers in vacuum. In aqueous solution, two conformers dominate at equilibrium. The preferred conformers superimpose well with the transition state structure, as determined previously for glycosyltransferase GnT-I. The conformations of **2** in the active site of glycosyltransferase GnT-I were obtained by docking methods. It was found that one of the two best docking poses mimics the binding mode of TS. These results suggest that the proposed TS mimics **2** have the potential to be used as a scaffold for the design of TS analogue inhibitors.

Keywords: Glycosylation; Glycosyltransferases; Inhibitors; Transition state analogues; Density functional theory calculations; Docking; Carbohydrates; Enzymes; Conformation analysis.

Glycosyltransferases are enzymes which transfer monosaccharides from a donor to a specific acceptor, which can be a protein, a lipid or another saccharide. The result of this catalytic reaction is the formation of a new glycosidic linkage[1–4]. The glycosylation reaction, conducted by glycosyltransferases, is one of the crucial biological processes for the post-translational modification of proteins and lipids. The reaction greatly influences various molecular recognition processes, including bacterial and viral infections, cell adhesion in inflammation, development, regulation, and many other intercellular communications and signal transductions[5–7]. The fact that changes in protein glycosylation are early indicators of cellular changes in many diseases makes inhibitors of glycosyltransferases promising leads with a potential for many therapeutic applications, such as in the

Collect. Czech. Chem. Commun. 2008, Vol. 73, No. 5, pp. 591–607

doi:10.1135/cccc20080591

treatment of cancer, inflammations, and viral infections[8,9]. Therefore, the development of glycosyltransferase inhibitors has recently gained increasing interest[10–12]. Attempts to develop potent inhibitors of glycosyltransferases were mostly based on mimicking the structure of natural substrates, but only a few of them exhibit a significant potency. Some of the intrinsic features of glycosyltransferases make creating rational designs of glycosyltransferase inhibitors a very difficult task. One feature is the weak binding of natural substrates to the enzyme that can be expressed in terms of millimole range of K_m values.

It is generally assumed that transition-state (TS) analogues of an enzyme-catalyzed reaction are the best inhibitors[13–15]. A transition-state analogue is defined as a stable compound that structurally resembles the three-dimensional structure and charge distribution of a substrate(s) portion of the unstable TS of an enzymatic reaction. Therefore, a prerequisite for the design of TS analogues is the understanding of the catalytic mechanism and, consequently, the structure of TS. In glycosyltransferases the transition state is a complex structure, in which three partners participate, namely an enzyme, a donor, and an acceptor. The metal ion, which binds a donor, is also often required for the activity of glycosytransferases[4].

In our previous studies, the catalytic mechanism was investigated and major structural features of the TS were determined for inverting glycosyltransferases[16–18]. Density functional theory (DFT) calculations using the truncated 127 atoms active site model[17], based on the X-ray crystallographic structure[19] of the uridinediphosphate-*N*-acetylglucosamine: α-1,3-D-mannoside β-1,2-*N*-acetylglucosaminyltransferase I (*N*-acetylglucosaminyltransferase I, GnT-I, EC 2.4.1.101), revealed one transition state associated with a reaction pathway following a concerted mechanism. GnT-I is an inverting family 13 glycosyltransferase that catalyzes the transfer of a GlcNAc residue (2-acetamido-2-deoxy-α-D-glucopyranose) from the nucleotide-sugar donor UDP-GlcNAc [uridine 5′-(2-acetamido-2-deoxy-α-D-glucopyranosyl pyrophosphate)] to the acceptor, which is the C2-hydroxy group of a mannose residue in the trimannosyl core of the $Man_5GlcNAc_2$-Asn-X oligosaccharide (Fig. 1). Later, the structure of the transition state (Fig. 2) for the reaction catalyzed by GnT-I was refined[18] using the hybrid quantum mechanics/molecular mechanics methodology (QM/MM), in which the full system (GnT-I plus substrates) was allowed to relax. Based on these results, the calculated models of transition states were clustered into three canonical forms[17]. These forms were termed using geometrical criteria based on the values of two reaction coordinates, the C1–O_{acc} and C1–O1 distances, as "early", "intermediate" or "late transition state", respectively. TS structures

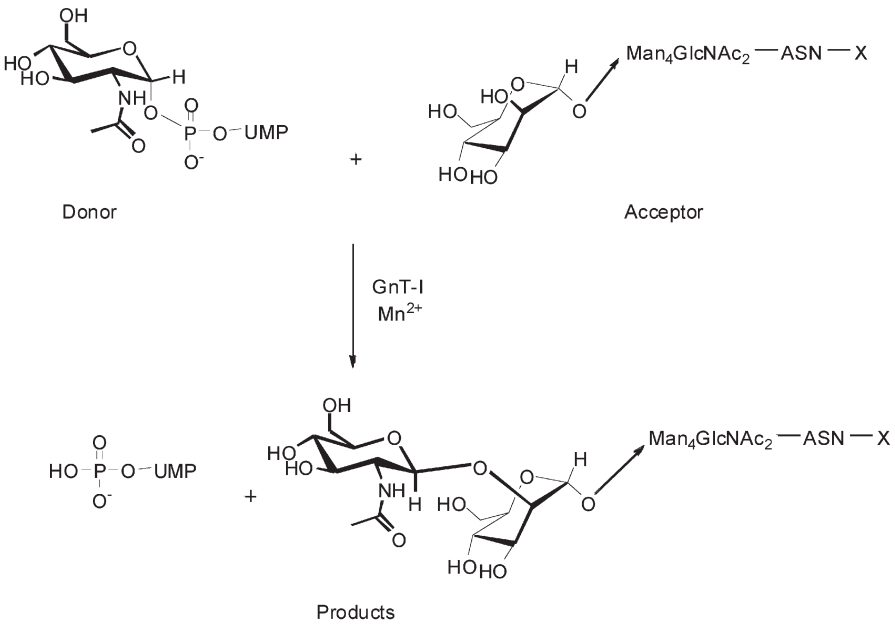

FIG. 1
Schematic diagram of the enzymatic reaction catalyzed by GnT-I

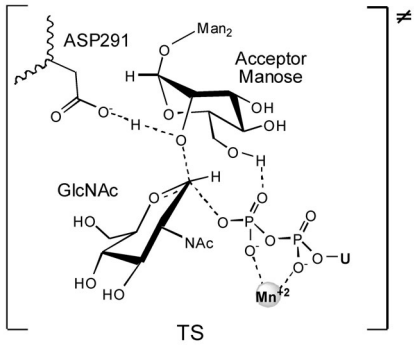

FIG. 2
Schematic representation of the TS for the GlcNAc transfer catalyzed by GnT-I

where both C1–O_{acc} (2.1–2.4 Å) and C1–O1 (2.5–2.7 Å) distances are elongated compared with their initial values, but where the structures did not yet reach their final arrangement in products, represent the "intermediate transition state" structures.

The analysis of calculated models of transition states[16–18] has led to the identification of key structural characteristics of the transition state that can be described as follows: (i) the hexopyranose ring conformation resembles a half-chair conformation with the oxocarbenium character at the anomeric carbon; (ii) the C1–O1 distance is considerably longer; (iii) a new β-glycosidic bond is being formed with the bond length larger than the normal bond length; the formed and cleaved bonds are oriented almost perpendicularly with respect to the plane defined by the C2–C1–O5 atoms of the pyranose ring. Designing a stable molecule that mimics the transition state narrowly is very difficult because of the above described characteristics of the TS. However, even crude TS analogues incorporating all relevant features are expected to be excellent reversible inhibitors[14].

Recently, we have proposed the [2-(methylsulfanyl)tetrahydrofuran-2-yl]-methyl phosphate dianion (**1**) as a scaffold for the transition state analogues[20]. A derivative of the proposed scaffold was synthesized[21] and is being tested against recombinant GnT-I glycosyltransferase[22]. The results of primary screening are very encouraging and prompt us to continue in designing of TS analogue inhibitors for glycosyltransferases. Here we propose a new scaffold, which is a modification of **1**, in which the phosphate anion is replaced by a sulfate anion. The new analogue should serve to increase the diversity of analogues that might later be used in the lead refinement process. In this paper, we investigate the structure, as well as the conformational and binding behavior, of the proposed compound.

METHODOLOGY

The schematic representation and labeling of atoms for the proposed TS analogue [(2*S*,3*R*,4*R*,5*S*)-3,4,5-trihydroxy-2-(phenylsulfanyl)tetrahydrofuran-2-yl]methyl sulfate anion (**2**) is in Fig. 3.

Jaguar program[23], version 5.5, was used for all calculations carried out in this study. First, an approximate estimate of the conformational behavior of **2** was obtained through a series of optimization calculations, using the density functional method (DFT) and B3LYP functional[24,25] at the 6-31+G* level for three dihedral angles describing rotation around anomeric linkages, C1–C8 and C1–S6, and rotation of the sulfate group around C8–O9 linkage. The three rotational degrees of freedom associated with the orien-

tation of the groups linked to the anomeric carbon atom can be expressed in terms of dihedral angles Φ = Φ[O5–C1–C8–O9], Ψ = Ψ[O5–C1–S6–C7], and ω = ω[C1–C8–O9–S10], respectively. The Φ and Ψ torsion angles were varied by 30° increments within the 0–360° range. For the ω angle, three values were used, namely ω = 60°, ω = –60°, and ω = 180°. The ω values correspond to +gauche (*G*), –gauche (*mG*), and trans (*T*) rotamers around the C8–O9 linkage. Except the dihedral angles of Φ, Ψ, and ω, all geometrical parameters were optimized during the calculations. Therefore, each calculated structure corresponds to the most stable geometrical conformation for the fixed values of Φ, Ψ, and ω. As a result, the total energy of **2** could be expressed as a function of the three torsion angles. The conformational properties were, therefore, demonstrated by means of three two-dimensional (Φ, Ψ) potential-energy surfaces (PESs), each corresponding to one of three values of ω. The PESs enabled determination of low-energy domains. For determination of minima, further optimizations without constraints on the three fixed dihedral angles were required.

The geometries of all identified local minima were, therefore, further subjected to such optimization, allowing full relaxation of the structures using a larger basis set, 6-311++G**. Consequently, vibrational frequencies for all minima of **2** were calculated at the B3LYP/6-31G* level using the modified scaled quantum mechanical force fields (SQM) method[26] for frequency scaling. Zero-point energy, thermal, and entropy corrections were evaluated using standard statistical thermodynamics methods based on the ideal-gas

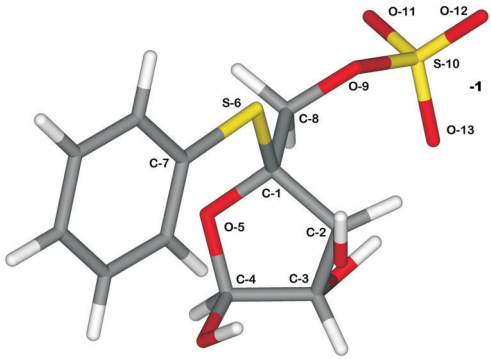

FIG. 3
Schematic representation and labeling of the atoms for the proposed [(2*S*,3*R*,4*R*,5*S*)-3,4,5-trihydroxy-2-(phenylsulfanyl)tetrahydrofuran-2-yl]methyl sulfate anion (**2**)

rigid-rotor model[27]. Then the solvent effects on conformational equilibria were investigated with a self-consistent reaction field method as implemented in the Jaguar program at the B3LYP/6-31+G* level, using the Poisson–Boltzmann solver[28,29]. The calculations were performed for water as the solvent, considering a dielectric permittivity of 80.37. Finally, the population of each conformer of **2** in the conformational equilibrium at 298 K was determined through the Boltzmann equation.

For the docking study, we have used the Glide program, a part of First Discovery 2.7 package[30] from Schrödinger. The Glide (grid-based ligand docking with energetics) program uses a hierarchical series of filters to search for possible locations of the ligand in the active-site region of the receptor. The shape and properties of the receptor are represented on a grid by several different sets of force fields which provide progressively more accurate scoring of the ligand poses. Conformational flexibility is handled in Glide by an extensive conformational search, augmented by a heuristic screen. For each core conformation, an exhaustive search for possible locations and orientations is performed over the active site of the protein. The scoring is carried out using Schrödinger's version of the ChemScore empirical scoring function[31]. This algorithm recognizes favorable hydrophobic, hydrogen-bonding, and metal–ligand interactions, and penalizes steric clashes. Description of Mn^{2+}-ligand interactions employs steric and electrostatic terms. Finally, the minimized poses are rescored using Schrödinger's proprietary GlideScore scoring function. The GlideScore is based on the ChemScore, but includes a steric-clash term and adds buried polar terms devised by Schrödinger to penalize electrostatic mismatches. The choice of the best-docked structure for each ligand is made using the GlideScore.

Crystallographic structure data[19] of GnT-I were used for the docking studies and for the investigation of enzyme–ligand interactions. The GnT-I structure was prepared by adding missing hydrogen atoms to the protein structure by the protein preparation routine implemented in First Discovery. Then grid generation for the active site was performed. The binding site was defined on the basis of the available crystal structure of the enzyme–donor complex. The center of a box, which defines the active site, was placed on the center of mass of the bound donor. The box size was set to 14 Å in all three dimensions. During the grid generation, the parameters for van der Waals radii scaling were scaled by 1.00 for atoms with a partial atomic charge less than 0.25, and no constraints were defined. Conformers of the analogue **2** were docked into the generated grids. We used flexible docking with single precision. During the docking procedure, the OPLS2001 partial atomic charges were assigned for the analogue **2**. The pa-

rameters for van der Waals radii scaling in docking were scaled by 0.80 for atoms with a partial atomic charge less than 0.15. The predicted poses were clustered within root mean square deviation less than 0.5 Å and within maximum atomic displacement less than 1.3 Å. After the docking procedure, 20 poses with the best score were saved and used for the analysis. Docking results were analyzed with Glide pose viewer[30].

RESULTS AND DISCUSSION

A starting structure of the proposed analogue **2** that is used for further calculations has been generated by the optimization carried out without constraints at the B3LYP/6-31+G* level. In the calculated structure of **2**, characteristic geometric features of the TS are represented as follows: the enlarged C1–O1 distance presented in the TS is accomplished by linking a methyl sulfate group to C1. In this moiety, the C1–O9 distance between the anomeric carbon and the sulfate oxygen is 2.5 Å, which is very close to the corresponding distance in the TS; the length of the C1–S6 bond is 1.9 Å, similar to the distance between the anomeric carbon and the attacking oxygen in the TS; the C1–C7 distance 2.9 Å corresponds to its distance in the TS. A distorted monosaccharide ring in the TS is represented by a five-membered ring. The bond angle C8–C1–S6 is close to 110°, which is less than in the TS. However, mimicking the almost linear arrangement of substituents (the leaving and attacking oxygen atoms) at the anomeric center (O–C–O angle) in the TS is very difficult, if not impossible. Nevertheless, as expected, the geometry of **2** is quite similar to that of **1**.

The available conformational space of **2** was monitored by means of three two-dimensional (Φ, Ψ) potential-energy surfaces, each of them corresponding to a fixed value of the torsional angle ω, and describing the orientation of the sulfate group. The three ω values used were 60° (*G*), –60° (*mG*), and 180° (*T*). The emphasis on exploring the conformational space in Φ- and Ψ-directions resulted from the fact that both the phenylsulfanyl and methyl sulfate groups are linked to the same carbon, causing additional complications in establishing the equilibrium conformation of the individual groups. Despite incomplete inspection of the conformational space in the ω-direction, this procedure provided a reasonable scan of the available conformational space and the representative number of conformers, altogether 432, was calculated.

The calculated B3LYP/6-31+G* conformational-energy maps are shown in Fig. 4. The symbols M1–M8 depicted on the maps indicate eight low-energy domains. The map of *G* rotamer (ω ~ 60°) around the C8–O9 bond contains

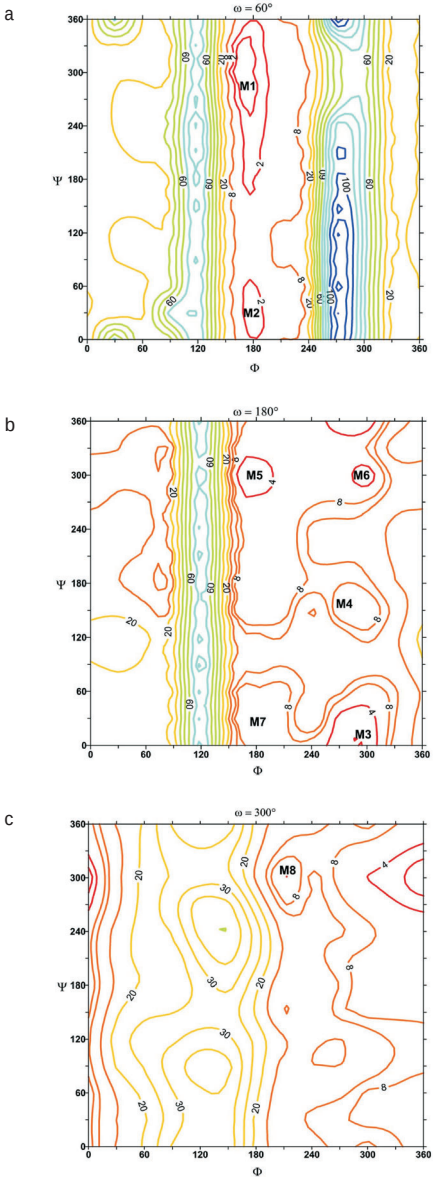

FIG. 4

Relaxed conformational-energy maps of [(2*S*,3*R*,4*R*,5*S*)-3,4,5-trihydroxy-2-(phenylsulfanyl)-tetrahydrofuran-2-yl]methyl sulfate anion (**2**) calculated at the B3LYP/6-31+G* level as a function of the torsion angles Φ and Ψ, with the torsion angle ω in *G* (a), *T* (b) and *mG* (c) orientation, respectively. The symbols M denote local minima

two of these regions (Fig. 4a), M1 and M2, having the (Φ, Ψ) values of ca. (180°, 270°) and (180°, 30°), respectively. Five regions M3–M7 (Fig. 4b), (300°, 0°), (300°, 150°), (180°, 300°), (300°, 300°), and (180°, 30°), respectively, were identified on the map for the *T* rotamer (ω ~ 180°). The last low-energy region M8 (Fig. 4c), (210°, 300°), was found for the *mG* rotamer (ω ~ –60°). The maps reveal an influence of interactions between the two groups linked to the anomeric carbon in the available conformational space of **2**. The rotation around the C1–C8 bond in the range 90–150° seems to be decisive in restricting the conformational space. Although the +gauche conformation corresponds to a local minimum of the individual C–S and C–C bonds[32], none of the maps shows a low-energy region in the (60°, 60°) area. The same conclusion was drawn for [2-(methylsulfanyl)tetrahydrofuran-2-yl]methyl phosphate dianion[20] (**1**) as a potential TS analogue.

The geometry optimization of local minima have been carried out at the B3LYP/6-311++G** level with full relaxation, including previously fixed torsional angles Φ, Ψ, and ω. The resulting minima were used to determine the most populated conformations and to reveal their structural details. The optimized values of the Φ, Ψ, and ω dihedral angles and other selected angles [τ_1 = τ(C4–O5–C1–S6), τ_2 = τ(C4–O5–C1–C8), τ_3 = τ(C4–O5–C1–C2), and α = α(S6–C1–C8)] of eight resulting conformers are given in Table I. The relative energies of the calculated minima in vacuum and in aqueous

TABLE I
Comparison of the B3LYP/6-311++G** calculated geometrical parameters (in °) for conformers of the [(2*S*,3*R*,4*R*,5*S*)-3,4,5-trihydroxy-2-(phenylsulfanyl)tetrahydrofuran-2-yl]methyl sulfate anion (**2**)

Conformer	Φ	Ψ	ω	τ_1	τ_2	τ_3	α	Ring
M1	–178.9	–81.9	93.7	–117.4	120.3	–1.0	112.5	E_3
M2	178.8	30.6	96.2	–129.0	116.1	–6.9	112.1	$^2T_3$
M3	–72.7	19.5	–172.1	–120.3	126.0	1.2	102.5	E_3
M4	–80.8	167.3	–120.9	–113.8	131.7	8.0	108.3	$^4T_3$
M5	–162.5	–68.9	–165.1	–77.1	157.1	37.9	112.6	^1E
M6	–71.1	–69.4	–127.3	–104.7	134.4	2.8	109.8	$^4T_3$
M7	–175.5	25.5	119.1	–128.8	115.2	–7.3	105.4	$^2T_3$
M8	–135.4	–67.1	–93.8	–77.5	158.0	36.3	113.5	^1E

solution, as well as the estimated populations for each conformer at equilibrium at 298 K, are summarized in Table II. These data clearly illustrate the profound influence of solvent on the equilibrium mixture. In vacuum, the conformers M1, M4, M7, M8, M2, and M6 of **2** are present at equilibrium, contributing to the overall composition by 48.7, 29.5, 8.8, 8.8, 2.8, and 1.5%, respectively. On the contrary, the number of conformers of **2** in aqueous solution decreases to two. These conformers do not correspond to the two most abundant found in vacuum. In aqueous solution, M8 is the dominant conformer (77.45%) and is accompanied by the conformer M5 (22.51%). The orientation around the C1–S6 and C1–C8 linkages of the most abundant conformers in vacuum and in aqueous solution, M1 and M4 versus M8 and M5, respectively, is characterized by either the *T* or *mG* orientation. The structural features of these conformers are illustrated in Fig. 5. On the other hand, the *G* orientation occurs in conformers with low or negligible population. The results indicate differences in preference for the orientation around C–X anomeric bonds between the five- and six-membered rings. The situation in the six-membered ring, which is influenced by the exo-anomeric effect[33], has been previously investigated in detail[32] and the preference for the gauche over trans conformation has been observed for the C1–X bond in *C*- and *S*-glycosyl compounds.

Another feature of the TS analogue **2** that can influence its inhibitor potency against GnT-I is the furanose ring conformation. The five-membered furanose ring is more flexible than the six-membered pyranose ring and can adopt several ring forms. The furanose ring conformation is influenced, among others factors, by the character and orientation of the ring substituent. Exploration of all possible ring shapes for all combinations of orientation of ring substituents would be too time consuming. Therefore, in this study the ring geometrical variables were fully optimized without constraints for each calculated PES point. The calculated results show how the furanose ring conformation is affected by the orientation of its substituents (Table I). Several configurations were predicted for the optimized local minima M1–M8. In vacuum, the furanose ring adopts the E_3, $^4T_3$, $^2T_3$, ^1E, $^2T_3$, and $^4T_3$ forms in minima M1, M4, M7, M8, M2, and M6, respectively. In aqueous solution, on the other hand, the equilibrium is completely shifted towards the ^1E ring conformer. It is noteworthy that the M8 and M5 conformers encompassing the ^1E form have also the largest values of angle α (S6–C1–C8), 113.5 and 112.6°, respectively. Although the arrangement of substituents on the anomeric carbon is far from linear, the preference for larger α values in solution makes these conformers promising TS analogues for inverting glycosyltransferases.

TABLE II

Comparison of the calculated relative energy (ΔE), zero point energy (ZPE), entropy (ΔS), thermal energy corrections (ΔH), Gibbs solvation energy (E_{solv}), Gibbs energy in vacuum and aqueous solution (ΔG_{gas}, ΔG_W) and estimated equilibrium percentages (x) of the [(2*S*,3*R*,4*R*,5*S*)- 3,4,5-trihydroxy-2-(phenylsulfanyl)tetrahydrofuran-2-yl]methyl sulfate anion (**2**) conformers

Conformer	ΔE kcal/mol	ZPE kcal/mol	ΔS cal/mol K	ΔH_{298} kcal/mol	ΔG_{gas} kcal/mol	x_{gas} %	E_{solv} kcal/mol	ΔG_W kcal/mol	x_W %
M1	1.34	151.78	142.51	12.36	0.00	48.7	–63.05	11.37	0.0
M2	1.17	151.90	134.12	11.60	1.69	2.8	–61.96	12.00	0.0
M3	3.53	151.69	130.31	11.18	4.55	0.0	–65.24	6.34	0.0
M4	0.70	152.09	140.08	12.26	0.30	29.5	–61.41	12.83	0.0
M5	4.73	151.35	135.44	11.58	4.28	0.0	–67.97	0.73	22.5
M6	2.08	151.47	134.10	11.50	2.08	1.5	–66.11	4.48	0.0
M7	0.00	152.05	132.71	11.52	1.01	8.8	–62.79	10.19	0.0
M8	1.93	151.55	138.65	11.87	1.02	8.8	–67.69	0.00	77.5

The binding properties of TS analogues are mainly determined by structural similarity between the transition-state and its analogue. To further evaluate the potential of **2** to mimic TS, a set of conformers, obtained from DFT conformational analysis, were superimposed into the calculated structure of the TS model and docked into the active site of GnT-I. The superimposition of the calculated conformers with the TS structures using the atom fit alignment of the most relevant atoms, i.e., sulfur S6 with the attacking

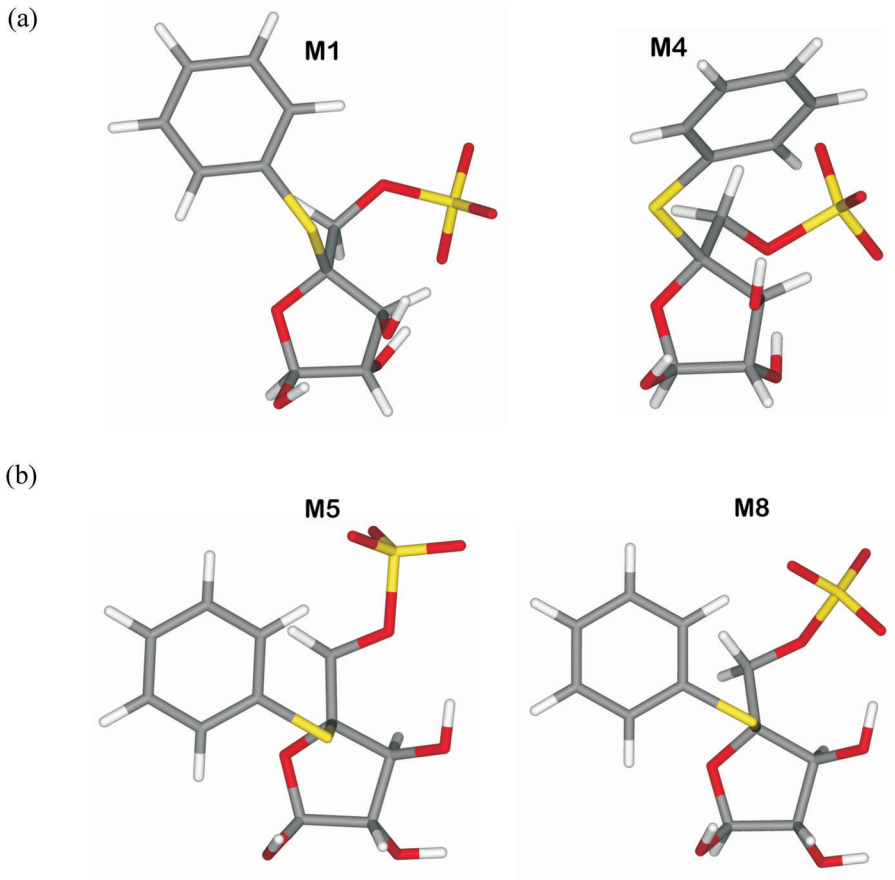

FIG. 5
Comparison of the B3LYP/6-31++G** calculated three-dimensional structures of the preferred conformers of the [(2*S*,3*R*,4*R*,5*S*)-3,4,5-trihydroxy-2-(phenylsulfanyl)tetrahydrofuran-2-yl]-methyl sulfate anion (**2**) in vacuum (M1, M4) (a) and in aqueous solution (M5, M8) (b)

oxygen O2 and the sulfate S10 with the phosphate P of the leaving group of the donor, implies that most of the calculated conformers mimic the corresponding parts of the TS structure well. An example of a superimposition is illustrated in Fig. 6. A reasonable overlap of the dominant conformer in aqueous solution, M8 with the TS structure, supports our assumption that the proposed scaffold **2** may adopt conformations that have very similar structural features to those predicted for TS of reactions catalyzed by inverting glycosyltransferases. This good alignment also implies a possibility of interactions between the sulfate group and the bivalent metal cofactor in the active site of the enzyme.

Glycosyltransferase GnT-I belongs to the GT-A superfamily, with the catalytic site located near the Rossmann-type fold. The crystal structure of GnT-I showed that the active site contains the catalytic base, the divalent metal cofactor Mn^{2+}, the so-called DxD motif (the amino acid motif which serves to bind the metal cofactor and which is standard for the whole GT-A family) present in the form Glu211-Asp212-Asp213 (^{211}EDD^{213}), and several other amino acids involved in substrates binding. Since the phosphates of the nucleotide sugar (donor, UDP-GlcNAc) coordinate the Mn^{2+} ion, the relative orientation of the donor is well defined within the enzyme–substrate complex. In the TS model, the interactions between the diphosphate group and the metal ion are preserved. Therefore, it is assumed that interactions between the Mn^{2+} ion and TS analogues would also be expected to play an

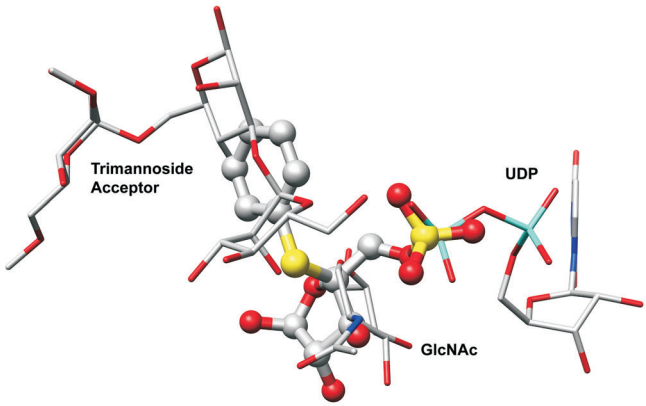

FIG. 6
Superposition of the predicted TS structure[18] and the M8 conformer of the [(2*S*,3*R*,4*R*,5*S*)-3,4,5-trihydroxy-2-(phenylsulfanyl)tetrahydrofuran-2-yl]methyl sulfate anion (**2**)

important role in inhibitor binding. For analogue **2**, docking was carried out with the program GLIDE, and the best docked poses were analyzed. Inspection of docking revealed the presence of two main binding poses with the same GlideScore of –9.2.

In both poses, analogue **2** was found to fit nicely into the active site of GnT-I, with the sulfate group buried deeply in the vicinity of the Mn^{2+} ion. This is also reflected in a number of interactions between GnT-I and **2**. An analysis of these interactions shows that interactions of the sulfate group with the Mn^{2+} ion are very similar in both poses. The calculated O11–Mn and O13–Mn distances are 1.918 and 3.154 Å in the first pose and 3.733 and 1.909 Å in the second pose, respectively. The calculated O–Mn distances imply strong electrostatic interactions, which explain their higher affinity when compared with other docked poses. However, in spite of the similar sulfate–Mn^{2+} interactions, two poses have altered binding modes (Fig. 7) and the position and interactions of the rest of **2** with the enzyme differ in both poses. In the first pose (Fig. 7, yellow), the furanose ring is positioned in the location of the transferred GlcNAc and its hydroxy groups form two strong hydrogen bonds with the enzyme. The phenyl group is placed in an *N*-acetyl binding pocket and stacking interactions with Leu 269 contribute to the binding energy. The bonded conformation is characterized by the dihedral angles Φ, Ψ, and ω, equaling –51, –47, and 146°, respectively. In the second pose (Fig. 7, green), the structure is positioned in

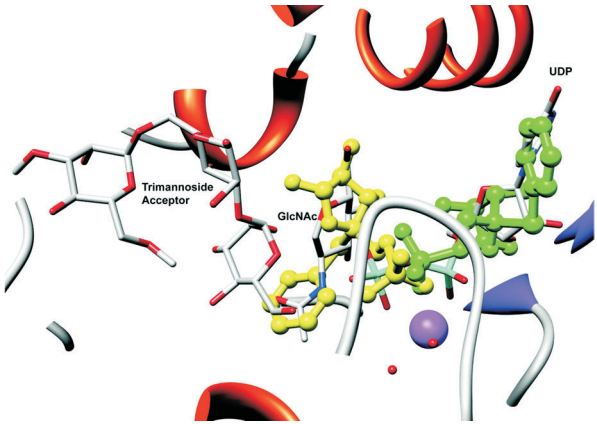

FIG. 7
Two predicted binding poses of **2** obtained by GLIDE superimposed on the TS structure[18] in the active site of the crystal structure of GnT-I

the binding place for the UDP part of UDP-GlcNAc, mimicking some donor– substrate interactions. The phenyl group is located in the uridine position and the sugar-mimicking part is found at the ribose place. Hydroxy groups on the furanose ring make two hydrogen bonds with the enzyme, the phenyl group is in the hydrophobic pocket between Ile 187 and Val 321. This bonded conformation of **2** is characterized by the dihedral angles Φ, Ψ, and ω, equaling 45, –177, –134°, respectively. Inspection of values in Table II shows that bonded conformations are slightly different from the most stable conformations predicted for **2** in solution. DFT calculations of the bound structures in solution at the B3LYP/6-311++G** level gave the Gibbs energy differences with respect to the M8 conformer of 6.7 and 13.2 kcal/mol. However, such conformational changes are understandable and are often caused by interactions with the enzyme. The observed docking score imply better binding affinity for **1** (GlideScore –11.2) than that for **2** (–9.2).

These results suggest that **2** may serve as a scaffold for potential inhibitors of glycosyltransferases. Of course, there is room for improvement by elucidating further variations of its structure using modifications of substituents on the furanose ring. Certainly, a selection of suitable substituents mimicking the acceptor is of special interest, as this part might be a key factor influencing the specificity of inhibitors. In general, for every donor nucleotide there is a large number of possible acceptors, e.g. UDP-GlcNAc is the donor for at least 13 different GlcNAc glycosyltransferases involved in biosynthesis of *N*- and *O*-glycans, itself requiring 13 different acceptors. Therefore, it is assumed that the latter may define the specificity of inhibitors of a particular glycosyltransferase.

CONCLUSIONS

Investigation of the conformational behavior and binding properties of the [(2*S*,3*R*,4*R*,5*S*)-3,4,5-trihydroxy-2-(phenylsulfanyl)tetrahydrofuran-2-yl]-methyl sulfate anion (**2**), which mimics the TS of the inverting glycosyltransferases, suggests that **2** can be used as a scaffold for the design of TS analogue inhibitors. Conformational analysis of **2** has been carried out using a density functional theory method at the B3LYP/6-311++G** level, which led to finding six equilibrium conformers in vacuum and two dominant conformers in aqueous solution. The superimposition of conformers with the TS structure determined for glycosyltransferase GnT-I showed that **2** can mimic TS. The conformations of **2** in the active site were deter-

mined by docking methods revealing the two most preferred poses, showing altered binding patterns which mimic the binding mode of TS.

This work was supported by grants from EC under contract MRTN-CT-2004-005645, and the Science and Technology Assistance Agency under contract APVT-51-004204.

REFERENCES

1. Beyer T. A., Sadler J. E., Rearick J. I., Paulson J. C., Hill R. L.: *Adv. Enzymol.* **1981**, *2*, 23.
2. Schachter H.: *Curr. Opin. Struct. Biol.* **1991**, *1*, 755.
3. Montreuil J., Vliegenthart J. F. G., Schachter H. in: *Glycoproteins* (A. Neuberger and L. L. M. van Deenen, Eds), Vol. 29a. Elsevier, Amsterdam 1995.
4. Wilson I. B. H., Breton C., Imberty A., Tvaroška I. in: *Glycoscience Chemistry and Chemical Biology* (B. O. Fraser-Reid, K. Tatsuta, J. Thiem, G. L. Coté, S. Flitsch, Y. Ito, H. Kondo, S. Nishimura and B. Yu, Eds). Springer-Verlag, Berlin 2008.
5. Maseras F., Morokuma K.: *J. Comput. Chem.* **1995**, *16*, 1170.
6. Varki A.: *Essentials of Glycobiology*. Cold Spring Harbor Laboratory Press, New York 1999.
7. Dennis J. W., Granovsky M., Warren C. E.: *BioEssays* **1999**, *21*, 412.
8. Dwek R. A.: *Chem. Rev.* **1996**, *96*, 683.
9. Dennis J. W.: *Semin. Cancer Biol.* **1991**, *2*, 411.
10. Wang R., Steensma D. H., Takaoka Y., Yun J. W., Kajimoto T., Wong C.-H.: *Bioorg. Med. Chem.* **1997**, *5*, 661.
11. Compain P., Martin O. R.: *Bioorg. Med. Chem.* **2001**, *9*, 3077.
12. Compain P., Martin O. R.: *Curr. Med. Chem.* **2003**, *3*, 541.
13. Pauling L.: *Am. J. Sci.* **1948**, *36*, 51.
14. Wolfenden R.: *Nature* **1969**, *223*, 704.
15. Schramm V. L.: *Annu. Rev. Biochem.* **1998**, *67*, 693.
16. Tvaroška I., Andre I., Carver J. P.: *J. Am. Chem. Soc.* **2000**, *122*, 8762.
17. Tvaroška I., Andre I., Carver J. P.: *Glycobiology* **2003**, *13*, 559.
18. Kozmon S., Tvaroška I.: *J. Am. Chem. Soc.* **2006**, *128*, 16921.
19. Unligil U. M., Zhou S. H., Yuwaraj S., Sarkar M., Schachter H., Rini J. M.: *EMBO J.* **2000**, *19*, 5269.
20. Raab M., Kozmon S., Tvaroska I.: *Carbohydr. Res.* **2005**, *340*, 1051.
21. Csúsz B., Hirsch J., Koóš M., Mucha J., Tvaroška I.: *Chem. Pap.* **2008**, *63*, submitted.
22. Mucha J.: Unpublished results.
23. *Jaguar 5.5*, Release 11 (Schrödinger). Portland, Oregon 2004.
24. Becke A. D.: *Phys. Rev. A* **1988**, *38*, 3098.
25. Perdew J. P.: *Phys. Rev. B* **1986**, *33*, 8822.
26. Baker J., Jarzecki A. A., Pulay P.: *J. Phys. Chem. A* **1998**, *102*, 1412.
27. Cramer C. J.: *Essentials of Computational Chemistry. Theories and Models*. Wiley, Chichester 2002.
28. Tannor D. J., Marten B., Murphy R., Friesner R. A., Sitkoff D., Nicholls A., Ringnalda M., Goddard W. A., Honig B.: *J. Am. Chem. Soc.* **1994**, *116*, 11875.
29. Marten B., Kim K., Cortis C., Friesner R. A., Murphy R. B., Ringnalda M. N., Sitkoff D., Honig B.: *J. Phys. Chem.* **1996**, *100*, 11775.
30. *First Discovery 2.7* (Schrödinger). Portland, Oregon 2004.

31. Eldridge M. D., Murray C. W., Auton T. R., Paolini G. V., Mee R. P.: *J. Comput.-Aided Mol. Des.* **1997**, *11*, 425.
32. Tvaroska I., Carver J. P.: *J. Phys. Chem.* **1996**, *100*, 11305.
33. Tvaroska I., Bleha T.: *Adv. Carbohydr. Chem. Biochem.* **1989**, *47*, 45.